Active Layer Optimization for IMPATT Diode with Double Avalanche Region

ALEXANDER ZEMLIAK
Department of Physics and Mathematics
Puebla Autonomous University
Av. San Claudio y 18 Sur, Puebla, 72570
MEXICO

Abstract: - The analysis and optimization of the n^+pvnp^+ avalanche diode structure that includes two avalanche regions have been realized on basis of the nonlinear model. The phase delay which was produced by means of the two avalanche regions and the drift region v is sufficient to obtain the negative resistance for the wide frequency band. The admittance and energy characteristics of the DAR diode were analyzed in very wide frequency band from 30 up to 340 GHz. Output power level was optimized for the second frequency band near the 220 GHz.

Keywords: - Semiconductor microwave devices, internal structure optimization, DAR IMPATT diode.

1 Introduction

One of the principal problems of modern microwave electronics is the problem of the power generation of sufficient output level for the short wave interval of millimeter region. Modern semiconductor technology provides the possibilities for the fabrication of submicron structures with a complex doping profile. The IMPATT diodes of different structures are used very frequently in microwave systems. The single drift region (SDR) and the double drift region (DDR) IMPATT diodes are very well known and used successfully for the microwave power generation in millimeter region [1]. The characteristic optimization permits to obtain a very high output power level [2]. From the famous paper of Read the main idea to obtain the negative resistance was defined on the basis of the phase difference being produced between RF voltage and RF current due to delay in the avalanche build-up process and the transit time of charge carriers. The transit time delay of both types of diodes is the essential factor of the necessary phase conditions to obtain a negative resistance. However an IMPATT diode that has double avalanche regions (DAR) can produce an avalanche delay which alone can satisfy conditions necessary to generate microwave power [3, 4]. In this case the phase delay of the drift zone becomes subsidiary. The DAR diode can be defined for instance by means of the structure n+pvnp+ in Fig. 1. The characteristics of this diode were analyzed in [4]. The authors affirm that the diode active properties are produced in many frequency bands for any drift zone width and this width has an influence on the number of the frequency bands. The larger drift zone provokes more number of frequency bands. Unfortunately since the first invention of DAR IMPATT diode there are no any experimental data concerning the fabrication and/or experimental characteristics investigation of such a type of diode. We analyzed some properties of DAR IMPATT diode on basis of nonlinear model [5]. The results obtained on basis of this sufficiently precise model contradict to the before performed analysis on basis of the approximate models and show that only diode with a sufficiently short drift region can produce active power in three frequency bands. The admittance characteristics of the diode were analyzed in very wide frequency region. We suppose that the optimization of semiconductor structure of the DAR diode can improve the output characteristics of IMPATT diodes for the microwave generation.

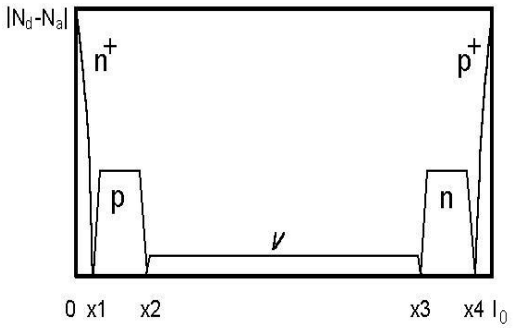

Fig. 1. Doping profile for DAR IMPATT diode.

2 Nonlinear Model and Optimization Technique

The drift-diffusion model which is used for the diode analysis describes all important physical phenomena of the semiconductor device. This model is based on system of two continuity equations for the electrons and holes, the Poisson equation for the potential distribution in semiconductor structure and necessary boundary conditions as for continuity equations and for the Poisson equation.

The DAR IMPATT diode model includes two differential equations for the carrier concentrations and two additional equations for current density definition. These equations are presented below in a normalized form:

$$\frac{\partial n(x,t)}{\partial t} = \frac{\partial J_n(x,t)}{\partial x} + \alpha_n \left| J_n(x,t) \right| + \alpha_p \left| J_p(x,t) \right|$$
$$\frac{\partial p(x,t)}{\partial t} = -\frac{\partial J_p(x,t)}{\partial x} + \alpha_n \left| J_n(x,t) \right| + \alpha_p \left| J_p(x,t) \right| \quad (1)$$
$$J_n(x,t) = n(x,t)\, V_n + D_n \frac{\partial n(x,t)}{\partial x}$$
$$J_p(x,t) = p(x,t)\, V_p - D_p \frac{\partial p(x,t)}{\partial x}$$

where n, p are the concentrations of electrons and holes; J_n, J_p are the current densities; α_n, α_p are the ionization coefficients; V_n, V_p are the drift velocities; D_n, D_p are the diffusion coefficients.

The dependences of the ionization coefficients α_n, α_p on field and temperature have been approximated using the approach described in [6]. The drift velocities and diffusion coefficients were calculated by means of approximations given in [7-9]. These approximations include all essential features of the carrier's mobility in silicon semiconductor structure and give possibility to calculate the diode behavior in a wide frequency band for the different regimes.

The boundary conditions for this system include concentration and current definition for contact points and can be written as follows:

$$n(0,t) = N_D(0); \qquad p(l_0,t) = N_A(l_0);$$
$$J_n(l_0,t) = J_{ns}; \qquad J_p(0,t) = J_{ps}. \quad (2)$$

where J_{ns}, J_{ps} are the electron current and the hole current for inversely biased *p-n* junction; $N_D(0)$, $N_A(l_0)$ are the concentrations of donors and acceptors at two end space points x=0 and x=l_0; where l_0 is the length of the active layer of semiconductor structure.

The electrical field distribution in semiconductor structure can be obtained from the Poisson equation. As electron and hole concentrations are functions of the time, therefore, this equation is the time dependent too and time is the equation parameter. The Poisson equation for the above defined problem has the following normalized form:

$$\frac{\partial E(x,t)}{\partial x} = -\frac{\partial^2 U(x,t)}{\partial x^2} = N_D(x) - N_A(x) + p(x,t) - n(x,t) \quad (3)$$

where $N_D(x)$, $N_A(x)$ are the concentrations of donors and acceptors accordingly, *U(x,t)* is the potential, *E(x,t)* is the electrical field. The boundary conditions for this equation are follows:

$$U(0,t) = 0; \quad U(l_0,t) = U_0 + \sum_{m=1}^{M} U_m \sin\left(\omega m t + \varphi_m\right) \quad (4)$$

where U_0 is the DC voltage on diode contacts; U_m is the amplitude of harmonic number m in diode contacts; ω is the fundamental frequency; φ_m is the phase of harmonic number m; M is the number of harmonics. In this paper we analyze one harmonic regime only ($M=1$) and in this case the phase φ_m can be define as 0. Concrete values of the voltages U_0, U_1 and frequency ω have been defined during the analysis in section 3. Equations (1)-(4) adequately describe the processes in the IMPATT diode in a wide frequency band. However, numerical solution of this system of equations is sufficiently difficult due to existing of a sharp dependence of equation coefficients on electric field. Explicit numerical schemes have poor stability and require a lot of computing time for good calculation accuracy obtaining. It is more advantageous to use implicit numerical scheme that has a significant property of absolute stability [10]. Computational efficiency and numerical algorithm accuracy are improved by applying the space and the time coordinates symmetric approximation. After approximation of functions and its differentials the system (1) is transformed to the non-evident modified Crank-Nicholson numerical scheme and has been solved by decomposition method for three-diagonal matrix.

The numerical scheme for the problem (1)-(4) solution for the different DDR IMPATT diode structures has been made and analyzed some years ago [11]. This analysis showed good convergence of the numerical model. The numerical algorithm convergence i.e. the physical processes stationary mode appearance was obtained during 6 – 8 high frequency periods. The analysis of numerical model for the DAR diode with the doping profile in Fig.1 shown [5] that the numerical scheme convergence for this type of the doping profile is very slow and the numerical transition process continues many periods to obtain the stationary mode. The necessary number of the consequent periods depends on the diode width and operating frequency and changes from 30 – 50 for the frequency band 15 – 60 GHz up to 150 – 250 periods for 200 – 300 GHz. This very slow convergence was stipulated by the asynchronies movement of the electron and hole avalanches along the same drift region *v*. It occurs owing to the different drift velocities of the carriers. This effect provokes a large number of necessary periods and large computer time, but it is necessary to wait till the finish of transition process to obtain the correct diode characteristics. This is a specific feature of the analyzed type of diode structure.

To optimize the output characteristics of DAR diode it is necessary to use some kind of optimization method. The optimization algorithm that was used is combined by one kind of direct method and a gradient method. To obtain the better solution for the optimum procedure, it is necessary to analyze *N*-dimensional space for *N*=5. The principal vector of optimization parameters consists of five variables $y = (y_1, y_2, y_3, y_4, y_5)$, where the components will be defined below. The optimization algorithm can be defined by next steps:

1. Given as input two different approximations of two initial points y^0 and y^1.
2. At this points, we start with the gradient method, and have performed some steps. As a result, we have two new points Y^0 and Y^1. This process is reflected by the next equations:

$$y^{0,n+1} = y^{0,n} - d_n \cdot \nabla F\left(y^{0,n}\right),$$

$$y^{1,n+1} = y^{1,n} - d_n \cdot \nabla F\left(y^{1,n}\right), \tag{5}$$

$$n=0,1,\ldots,N\text{-}1, \quad Y^0 = y^{0,N}, \quad Y^1 = y^{1,N},$$

where *F* is the cost function, and, d_n is the parameter of the gradient method.

3. We draw a line through two these points, and perform a large step along this line. We have a new point y^{s+1}:

$$y^{s+1} = Y^s + a\left(Y^s - Y^{s-1}\right), \; s = 1, \tag{6}$$

where a is the parameter of the line step.

4. Then we perform some steps from this point by the gradient method, and obtain a new point Y^s:

$$y^{s,n+1} = y^{s,n} - d_n \cdot \nabla F\left(y^{s,n}\right), \tag{7}$$

$$s = s + 1, \; Y^s = y^{s,N}.$$

Then step 3 and 4 are repeated with the next values of index *s* (*s* = 2, 3,…).

This optimization algorithm cannot find the global maximum of the cost function, but only a local one. To obtain the confidence that we have the better solution of the optimum procedure, it is necessary to analyze *N*-dimensional volume in more detail. During the optimization process, it is very important to localize the subspace of the *N*-dimensional optimization space for more detailed analysis. Then this subspace can be analyzed carefully.

3 Results

The accurate analysis for DAR IMPATT diode has been made for different values of *p*, *n* and *v* region width and the different donor and acceptor concentration level. The analysis showed that the active properties of the diode practically are not displayed for more or less significant width of the region *v*. The same doping profile as in [4] gives the negative conductance for very narrow frequency band only as shown in Fig. 2 in conductance versus susceptance plot.

The solid line of this figure gives dependency for drift layer width W_v = 0.6 mm and the dash line for W_v = 1.5 mm. First dependency displays the diode active properties for one narrow frequency band from 50 GHz up to 85 GHz. Second admittance dependency for W_v = 1.5 mm gives very narrow one frequency band from 40 GHz up to 62 GHz with a vary small value of negative conductance *G*. In general the admittance behavior has a damp oscillation character but only first peak lies in

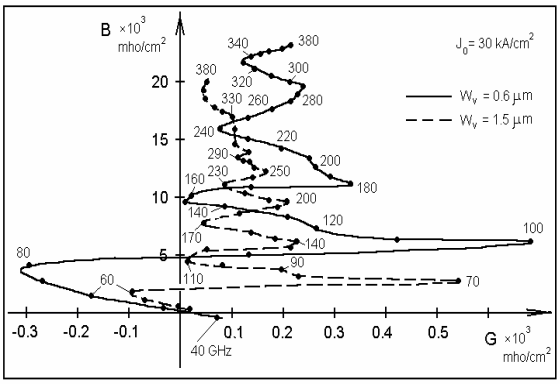

Fig. 2. Complex small signal DAR diode admittance (conductance -*G* versus susceptance *B*) for different frequencies and two values of drift layer widths W_v.

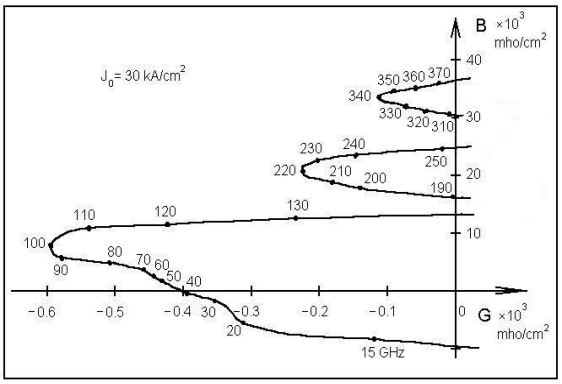

Fig. 3. Complex small signal DAR diode admittance (conductance -*G* versus susceptance *B*) for different frequencies and W_v = 0.32 μm.

negative semi plane. The negative conductance disappears completely for W_v >1.5 μm. All these results have been obtained in assumption of a sufficiently small value of a series resistance R_s = 0.5_{10}-6 Ohm · cm^2. This value was used for all further analysis too.

The main reason of obtained characteristics behavior is the same as for the slow mechanism convergence of the numerical model. The electron and hole avalanches have different transit velocities but they move along the same drift region *v*. It provokes different time delay for the carriers during the transit region movement. The larger width of the region *v* makes delay time more different and the active properties are reduced. That is why we need to reduce the width W_v to obtain necessary negative admittance. This conclusion is contrary to results of the paper [4]. The main results of the paper [4] showed the DAR diode active features presence in some frequency bands for different values of *v*-region widths from 0.5 μm to 2.0 μm. Our results display the active features of the DAR diode the same profile for some frequency bands in case when the *v*-region width less than 0.5 μm only.

One positive idea to increase negative admittance of the diode consists in non-symmetric doping profile utilization too. This profile gives some compensation to the asynchronies mechanism. Taking into account these considerations non-symmetric doping profile diode was analyzed in a wide frequency band. One of the perspective diode structures that was analyzed detail is defined by means of following parameters: the doping level of the *n*-zone is equal to $0.5_{10}17$ cm^{-3}, the doping level of the *p*-zone is equal to $0.2_{10}17$ cm^{-3}, the widths of the two corresponding areas are equal to 0.1 μm and 0.2 μm, accordingly, the width of the drift *v*-region is equal to 0.32 μm, the width of each *p-n* junction was given as 0.02 μm from the technological aspects. This structure provides concentration of electrical field within the two *p-n* junctions and asynchronies mechanism is not displayed drastically yet.

In Fig. 3 the small signal complex admittance i.e. the conductance versus susceptance is presented for the wide frequencies band for the above mentioned DAR diode and for the current density J_0 = 30 kA/cm^2. The DC voltage U_0 is equal to 26.59 V with a small variation from one frequency to other to obtain this value of current density. The first harmonic voltage amplitude is equal to 0.1 V.

There are some differences of the DAR diode frequency characteristics from the classical DDR IMPATT diodes. First of all this DAR diode type has three active bands in the millimetric range (Fig.3). The first active band of the DAR diode is very wide and covers frequency region from 12 to 138 GHz. The second and the third bands give the perspective to use this structure for the high frequency generation in the millimetric range too. We can decide that two superior bands appear from the positive conductance *G* semi plane (look Fig. 2) as a result of the special conditions making for these bands. This effect gives possibility to use superior frequency bands, at least the second band, for the microwave power generation of the sufficient level.

The maximum power density is equal to 37 kW/cm^2 for the first frequency band (90 GHz), and 1.4 kW/cm^2 for the second one (220 GHz). However possible optimization of the diode internal structure for selected frequency band can improve these

characteristics and permits to raise the power and the efficiency.

The DAR diode internal structure optimization has been provided below for the second frequency band near 220 GHz. The cost function of the optimization process was selected as output power level for the frequency 220 GHz. It means that the energy characteristics for the first and the third frequency bands have been obtained as functions of a secondary interest without a special improvement. The set of the variables for the optimization procedure was composed from five technological parameters of the diode structure: two doping levels for *p* and *n* regions and three widths of *p*, *n* and *v* regions. The optimal values of these parameters are following: doping level of the *n*-zone is equal to $0.42_{10}17$ cm^{-3}, the doping level of the *p*-zone is equal to $0.28_{10}17$ cm^{-3}, the widths of the two corresponding areas are equal to 0.1 μm and 0.2 μm, accordingly, and the width of the drift *v*-region is equal to 0.34 μm, The internal structure optimization of second frequency band has been made for the feeding current density 30 kA/cm^2. However it is interesting to calculate the diode power characteristics for other current density too. The complete analysis was done for three current density values: 30 kA/cm^2, 50 kA/cm^2 and 70 kA/cm^2. Although the structure optimization was provided for the large signal, the small signal diode admittance dependency is an interest too. These small signal characteristics are shown in Fig. 4 for all possible frequency bands and three values of feeding current density. The active diode properties for two first bands are improved when the current density increases.

Because the technological parameters have been optimized for 220 GHz more positive effect was obtained for this frequency. At the same time the third frequency band practically disappears. The maximum value of diode conductance for more favorable frequency 330 GHz of this band is equal to -30 mho/cm^2 for the structure optimized for the second band. On the other hand the diode conductance is equal to -120 mho/cm^2 for 340 GHz for before analyzed structure (Fig. 3).

The active diode properties for two first bands are improved when the current density increases. Because the technological parameters have been optimized for 220 GHz more positive effect was obtained for this frequency. At the same time the third frequency band practically disappears. The maximum value of diode conductance for more favorable frequency 330 GHz of this band is equal to -30 mho/cm^2 for the structure optimized for the second band. On the other hand the diode conductance is equal to -120 mho/cm^2 for 340 GHz for before analyzed structure (Fig. 3). Further current density increasing leads to complete disappearance of the active properties for this frequency.

The characteristics obtained for 220 GHz under the large signal serve as the main result of the optimization process. The amplitude characteristics for this frequency and for three values of feeding current density are shown in Fig. 5.

Because the diode structure optimization was provided for current density 30 kA/cm^2 the amplitude characteristic that corresponds to this current has better behavior in comparison to others.

This characteristic is softer. Characteristics for

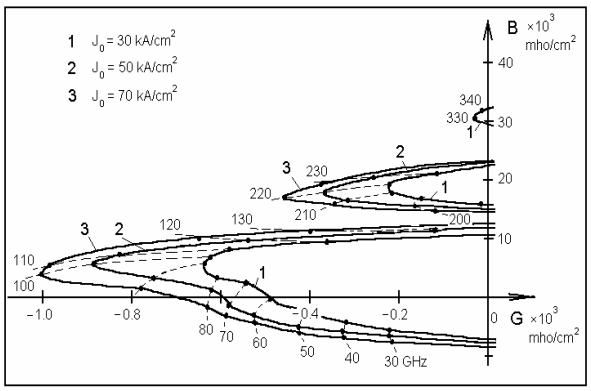

Fig. 4. Complex small signal DAR diode admittance optimized for second frequency band for different value of feeding current density.

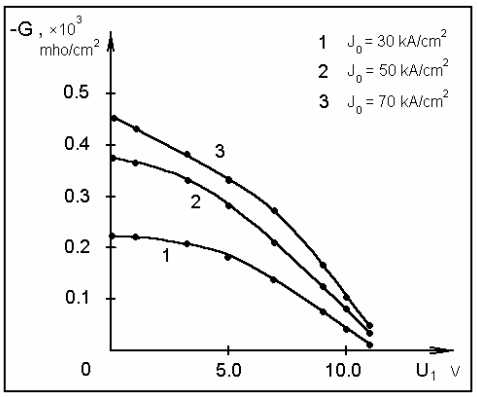

Fig. 5. Conductance *G* dependency as functions of first harmonic amplitude U_1 for f = 220 GHz and for three values of feeding current density.

the current densities 50 kA/cm^2 and 70 kA/cm^2 are sharper but correspond to the larger conductance $-G$. As a result this property gives a larger output power. The characteristics that correspond to two last current density values can be made better if the optimization process realize for each of this current value separately. The output power dependencies as a function of the first harmonic amplitude U_1 for f = 220 GHz and for three values of feeding current density are shown in Fig. 6.

We can state that a sufficient improvement of power characteristics is observed for this diode structure in comparison with before analyzed structure (Fig. 3). The maximum values of generated power are equal to 3.3 kW/cm^2 for J_0 =30 kA/cm^2, 6.0 kW/cm^2 for J_0 =50 kA/cm^2 and 7.5 kW/cm^2 for J_0 =70 kA/cm^2 accordingly. It is possible provide the diode structure optimization for the current density more than 30 kA/cm^2. In this case we can obtain a significantly more level of output generated power.

The analysis of the energy characteristic sensibility to the doping level and geometrical sizes for the current density J_0 =30 kA/cm^2 shown that the doping level variation within 15% around the optimal value leads to 3% output power decreasing. On the other hand the *p*, *n* and *v* region widths variation within 15% leads to 6-10% decreasing of output power level.

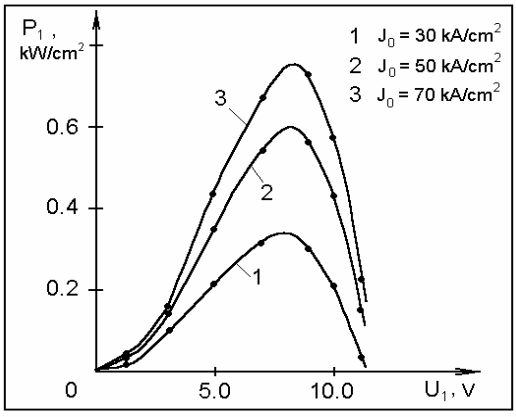

Fig. 6. Output generated power *P* dependency as functions of first harmonic amplitude U_1 for f = 220 GHz and for three values of feeding current density.

4 Conclusion

The numerical scheme that has been developed for the analysis of the different types of IMPATT diodes is suitable for the DAR complex doping profile investigation too. The additional problem of the numerical scheme slower convergence for the DAR diode can be overcome by the computer time increasing. The diode structure optimization gives the possibility to increase the output power level for the second frequency band up to 7.5 kW/cm^2. This level can be exceeding too by the special diode structure optimization taking into account necessary feeding current density.

Reference:

[1] G.I. Haddad, P.T. Greiling, and W.E. Schroeder, Basic principles and properties of avalanche transit-time devices, *IEEE Trans. Microwave Theory Tech.*, Vol. MTT-18, pp. 752-772., 1970.

[2] Chang K. (Ed.), *Handbook of microwave and optical components*, John Wile & Sons, New York, 1990.

[3] B. Som, B.B.Pal, and S.K.Roy, A small signal analysis of an IMPATT device having two avalanche layers interspaced by a drift layer, *Solid-State Electron*, Vol. 17, pp. 1029-1038, 1974.

[4] A.K. Panda, G.N. Dash, and S.P. Pati, Computer-aided studies on the wide-band microwave characteristics of a silicon double avalanche region diode, *Semicond Sci Technol*, No. 10, pp. 854-864, 1995.

[5] A. Zemliak, and R. De La Cruz, Computer Simulation of a Double Avalanche Regio n IMPATT Diode, *WSEAS Transactions on Circuits and Systems*, Vol. 3, No. 2, pp. 300-305, 2004.

[6] W.N. Grant, Electron and hole ionization rates in epitaxial silicon at high electric fields, *Solid-State Electron*, Vol. 16, No. 10, pp. 1189-1203, 1973.

[7] C. Jacoboni, C. Canali, G. Ottaviani, and A. Alberigi-Quaranta, A review of some charge transport properties of silicon, *Solid-State Electron*, Vol. 20, pp. 77-89, 1977.

[8] C. Canali, C. Jacoboni, G. Ottaviani, and A. Alberigi-Quaranta, High field diffusion of electrons in silicon, *Appl Phys Lett*, Vol. 27, p. 278, 1975.

[9] F. Nava, C. Canali, L. Reggiani, D. Gasquet, J.C. Vaissiere, and J.P. Nougier, On diffusivity of holes in silicon, *J Appl Phys*, Vol. 50, p. 922, 1979.

[10] A.M. Zemliak, Difference scheme stability analysis for IMPATT-diode design, *Izv. VUZ Radioelectron*, Vol.24, No.8, pp.831-834,1981.

[11] A. Zemliak, S. Khotiaintsev, and C. Celaya, Complex nonlinear model for the pulsed-mode IMPATT diode, *Instrumentation and Development*, Vol. 3, No. 8, pp. 45-52, 1997.